p-ISSN 2460-0768 e-ISSN 2597-6044 *GeoEco, Vol. 11, No 1. January 2025 Page. 62 – 72*
https://doi.org/10.20961/ge.v10i2.90987 https://jurnal.uns.ac.id/GeoEco/article/view/90987

COSEISMIC DEFORMATION OF THE 2020 BENGKULU MW 6.8 EARTHQUAKE USING INSAR DATA

Ongky Anggara*, and Satrio Muhammad Alif
Department of Geomatics Engineering, Institut Teknologi Sumatera, South Lampung, Indonesia

*E-mail: ongky.anggara@gt.itera.ac.id

ARTICLE INFO

Article History
Received : 23/07/24
Revised : 13/11/24
Accepted : 28/11/24

Citation:
Anggara, Ongky., and Alif, S.M., (2025) Coseismic Deformation Of The 2020 Bengkulu Mw 6.8 Earthquake Using Insar Data. Vol. 11, No. 1.

ABSTRACT

An earthquake with a seismic moment magnitude of Mw 6.8 occurred in Bengkulu province, located on the southwestern coast of Sumatra, on August 18, 2020. This study aims to assess the application of the differential interferometric synthetic aperture radar (DInSAR) method to detect and analyze coseismic deformation due to this earthquake using the Sentinel-1A radar satellite. The results of the DInSAR did not yield significant coseismic signals with the range of Line of Sight (LOS) displacement of ~-40 mm to ~40 mm. The InSAR data did not detect clear deformation patterns or displacements associated with the August 18, 2020 earthquake. Further investigations are needed to understand the limitations of InSAR in detecting coseismic signals for this specific event. Integrating these datasets can provide a more comprehensive understanding of the earthquake source, fault characteristics, and associated deformation patterns.

Keywords: *Bengkulu earthquake, Deformation, Coseismic, InSAR, Sentinel*

INTRODUCTION

The island of Sumatra, Indonesia, is located along the convergent boundary between the Indo-Australian Plate and the Sunda Plate, and the interaction between the two plates causes seismic activity. The region has experienced numerous earthquakes throughout history, including the devastating 2004 Aceh earthquake (Tanioka et al., 2006; Vigny et al., 2005) and the 2010 Mentawai earthquake (Ardika et al., 2015). These events highlighted studies on earthquake mechanisms, deformation tectonics, and the associated risks.

Recent advancements in geodetic techniques have provided valuable tools for studying and monitoring earthquake events. Assessment of earthquake coseismic displacement using the Global Navigation Satellite System (GNSS) (e.g., Alif et al., 2021; Anggara et al., 2024) and Interferometric Synthetic Aperture Radar (InSAR) (Meilano et al., 2021; Alif et al., 2024) are two prominent methods used to measure

crustal deformations associated with earthquakes. GNSS is one of the precise measurements of ground displacements, while InSAR provides high-resolution interferograms for mapping surface displacements (Albano et al., 2018; Anggara et al., 2023; Fang et al., 2019; Natadikara et al., 2023; Zhao et al., 2018).

Interferometric synthetic aperture radar (InSAR) is a powerful technology for measuring the complexity of earthquakes in spatial dimensions. It gives more precise information about the consequences of significant earthquake displacement (Li et al., 2021). Furthermore, the use of Sentinel-1 satellite data, known for spatial resolution and frequent times, is accurate and timely ground observations (Yang et al., 2019).

On August 18, 2020, an earthquake with a magnitude of Mw 6.8 in Bengkulu province located on the southwestern coast of Sumatra. These results are based on the processing using Sentinel 1A data with the method Differential Interferometry Synthetic Aperture Radar (DInSAR). The study aims to analyze the coseismic displacement resulting from the Bengkulu earthquake and assess its impact on the region using the DInSAR method.

MATERIALS AND METHODS

In this study, We used Sentinel 1A from ascending and descending tracks covering the study area, which were processed using the DInSAR method to determine the Bengkulu earthquake on August 18, 2020 (**Figure 1**). Processing using two pairs of images, namely the master and slave images, with acquiring images before and after the earthquake to estimate the coseismic phase of the earthquake. The DInSAR processing uses GMTSAR software (Sandwell et al., 2010). Generally, processing includes preprocessing, alignment, interferometry, filter/snap, and geocode stages. Image coregistration or image coregistration is a process that combines two SAR images consisting of a master and slave image into one layer.

The process of forming an interferogram is carried out after going through the image coregistration stage by multiplying the master image with the complex conjugate of the slave image. The coherence value in images ranges from 0–1; the higher the coherence value, the more identical the images are, and the highest coherence value is one

which indicates that the images are identical, while the lower the value is closer to 0, the more non-identical the pair of image.

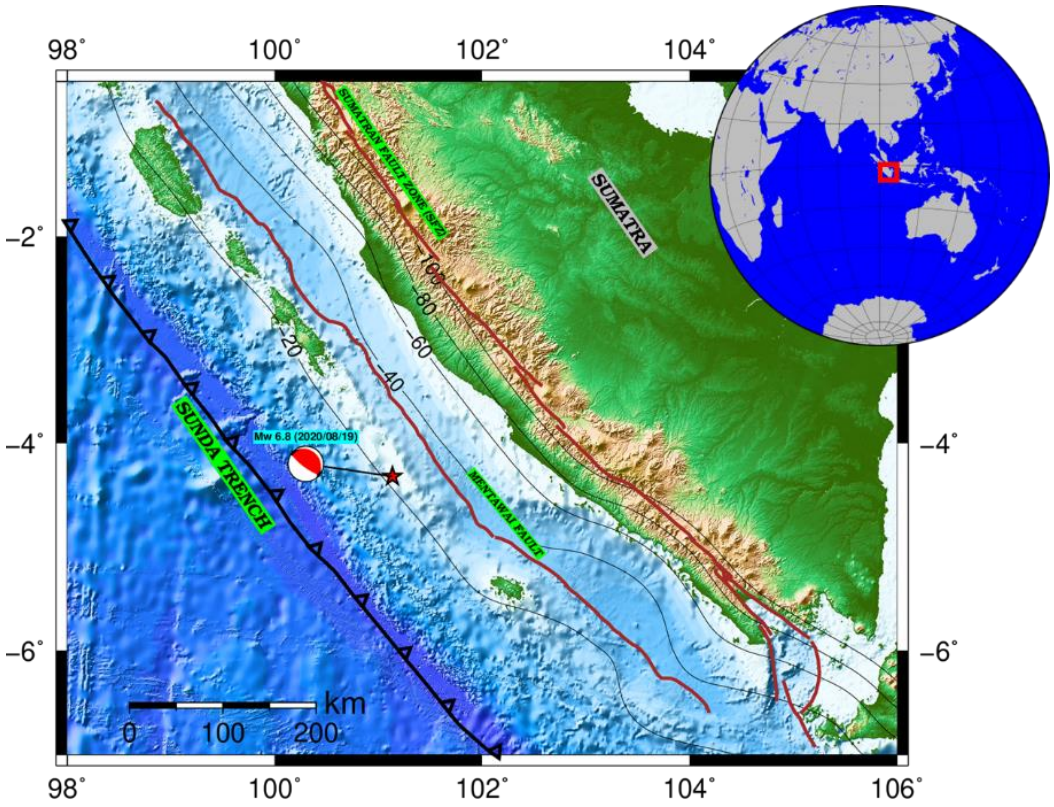

Figure 1. Location map of earthquake August 18 2020. The red star represented the epicentre of the earthquake in Bengkulu. Red beachball is the focal mechanism (Dziewonski et al., 1981). The Brown line represented the Fault of Mentawai Fault and Sumatran Fault Zone (PuSGeN, 2017)

In the DInSAR processing stage, the topography and filtering phases are removed. Topographic phase removal is carried out using SRTM 1-Arcsec DEM to remove topographic effects so that this process leaves displacement, atmospheric, and noise information. The filtering process was carried out using the advanced Goldstein filter method (Goldstein, 1998). Phase unwrapping changes the phase difference value of the master image and slave image into a deformation value (line of sight). The unwrapping process uses the SNAPHU algorithm (Chen & Zebker, 2002). Line of Sight (LOS) displacement is calculated using the following equation.

$$\text{LOS diplacement} = \frac{\theta\lambda}{-4\pi}$$

Where θ is the unwrapped phase difference, λ is the wavelength of the

Sentinel-1 satellite sensor (0.056 m). The Sentinel-1A level 1 (Single Look Complex) image data used was in the acquisition before and after the Bengkulu earthquake on August 18, 2020, with the Ascending and Descending satellite directions, each image pair was used in the process of determining the data that will be used as master and slave. In each image pair in **Table 1.** This study used 14 images that produced interferogram and line of sight (LOS) displacement images due to coseismic earthquakes. **Figure 2** shows the image acquisition footprint of sentinel 1A.

Table 1. Sentinel 1 image data acquisition

No	Satellite mission	Acquisition time	Orbit	Direction Satellite
1	Sentinel 1A	16/08/2020	91	Descending
2	Sentinel 1A	28/08/2020	92	Descending
3	Sentinel 1A	11/08/2020	18	Descending
4	Sentinel 1A	23/08/2020	18	Descending
5	Sentinel 1A	11/08/2020	18	Descending
6	Sentinel 1A	23/08/2020	18	Descending
7	Sentinel 1A	15/08/2020	69	Ascending
8	Sentinel 1A	27/08/2020	69	Ascending
9	Sentinel 1A	15/08/2020	69	Ascending
10	Sentinel 1A	27/08/2020	69	Ascending
11	Sentinel 1A	15/08/2020	69	Ascending
12	Sentinel 1A	27/08/2020	69	Ascending
13	Sentinel 1A	08/08/2020	142	Ascending
14	Sentinel 1A	20/08/2020	142	Ascending

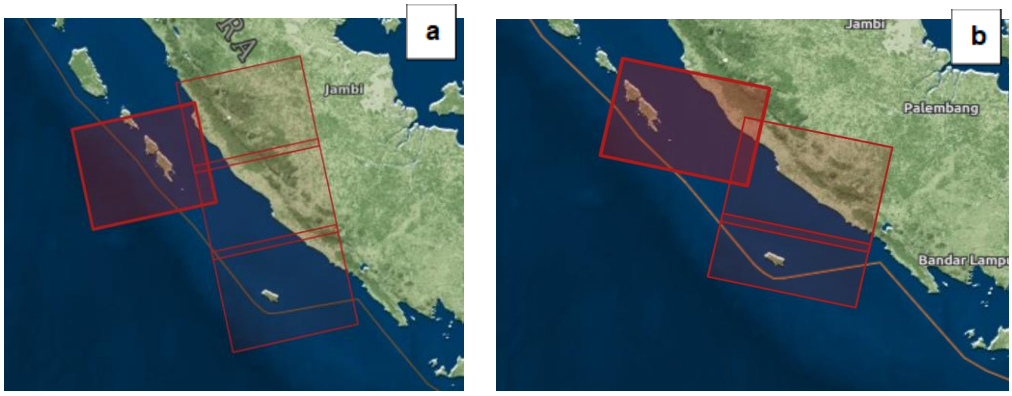

Figure 2. Acquisition of Sentinel-1A image data (a) ascending satellite direction (b) descending satellite direction

RESULTS AND DISCUSSION

In the coherence results, many areas have low values because the vegetation conditions are very dense, which affects the coherence results (Alif et al., 2023). High coherence values are defined with white colour values, while low coherence values are defined with black colour values. The decorrelation of interferometric signals is caused by differences in conditions between two SAR data acquisitions. These conditions include changes in the field's topography and atmospheric conditions (Amani et al., 2021). Another factor is decorrelation due to the addition of changes in the dielectric characteristics of scattering due to temporal factors and geometric factors of baseline decorrelation contained in the formation of interferograms using the DInSAR method (Jacob et al., 2020). Low correlation values are usually caused by the large amount of vegetation in the area (Suresh & Yarrakula, 2020). **Figure 3** shows the coseismic coherence of the August 18, 2020 Bengkulu earthquake.

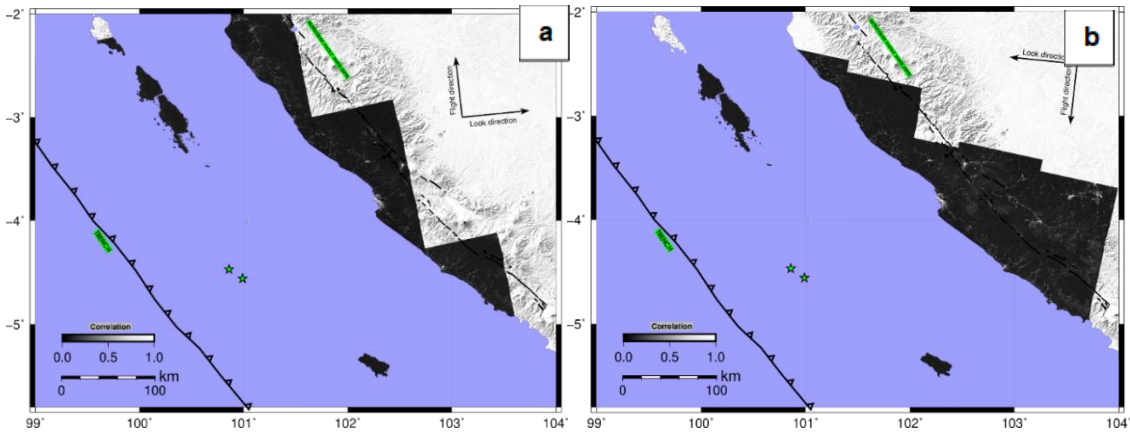

Figure 3. Coherence image pair (a) ascending direction (b) descending direction

The resulting interferogram fringes are represented in 2π wave cycles as colour cycles with a value range of -3.14 to 3.14 rad (**Figure 4**). Each cycle represents half a wavelength and represents relative ground displacement. The denser the fringes, the greater the deformation in the ground. In the coastal area of Bengkulu, denser fringes are visible, indicating a changing pattern. The ascending image has a better pattern, visible in parts of Enggano Island and South Pagai Island. The fringes are formed very well compared to the descending image. However, the dominant land area experiences

decorrelation. The interferogram that is formed greatly influences the earthquake's magnitude and the earthquake epicentre's distance to the image acquisition area. Sentinel 1 uses a limited C-band in imaging so that vegetation and dense residential objects will be distorted (Funning & Garcia, 2019).

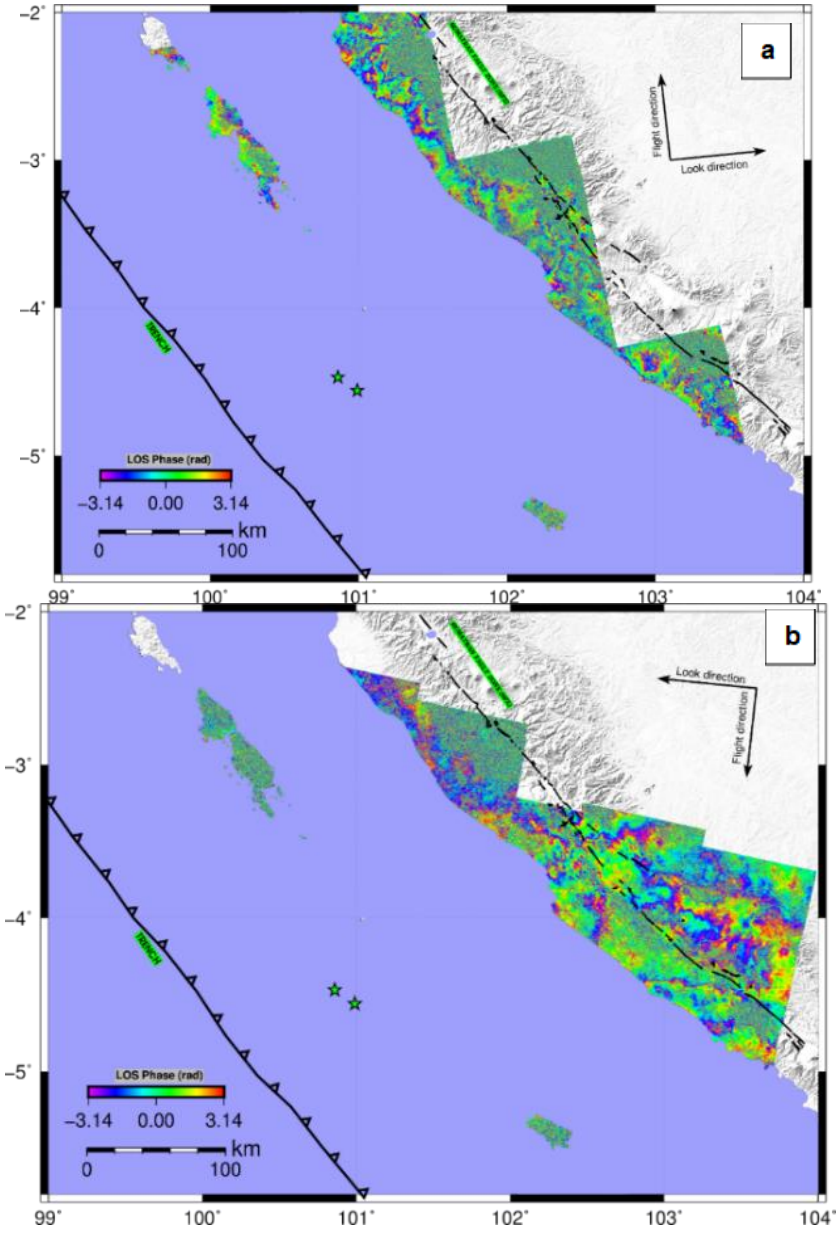

Figure 4. Interferogram Bengkulu earthquake August 18, 2020 (a) ascending direction (b) descending direction

The coherence and interferogram results are formed from pairs of images before and after the earthquake to determine the deformation that occurred by

unwrapping that the deformation phenomenon can be identified based on Line of Sight (LOS) displacement (Anggara et al., 2024). **Figure 5** shows the LOS Displacement in the direction of the ascending and descending satellite. The results of the Bengkulu coseismic earthquake with DInSAR on August 18 2020, with values ranging from ~-40 mm to ~40 mm with blue to red symbology. In the ascending LOS image, parts of Enggano Island and South Pagai Island experience deformation of ~-15 mm, while in the descending LOS image, there is deformation of ~15 mm. This difference is thought to be caused by different satellite directions. Radar images measure direction when the satellite is moving away with a negative value when the satellite direction is ascending, and the distance away from the object is compared with the direction of the descending image, which is moving closer to the object (Mora et al., 2016). However, the coherence and interferogram formed from the coseismic phase of the earthquake affect the Line of Sight (LOS) displacement results, which are influenced by the atmosphere (atmospheric disturbances) and phase unwrapping (Monterroso et al., 2020). These results are relevant to insar studies for small earthquakes by requiring estimates of non-tectonic contributions to ground displacement before estimating the geometry and kinematics of the earthquake source (Albano et al., 2018; Yu et al., 2018).

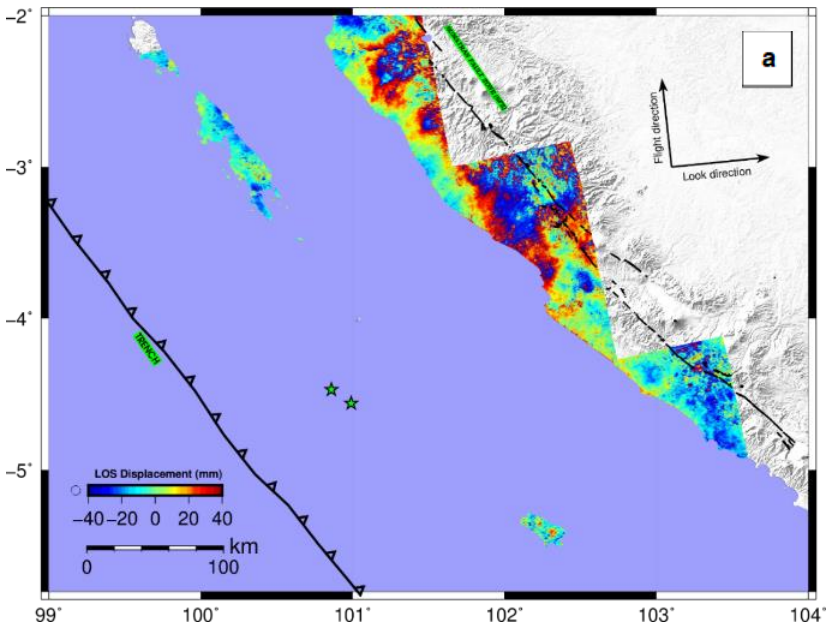

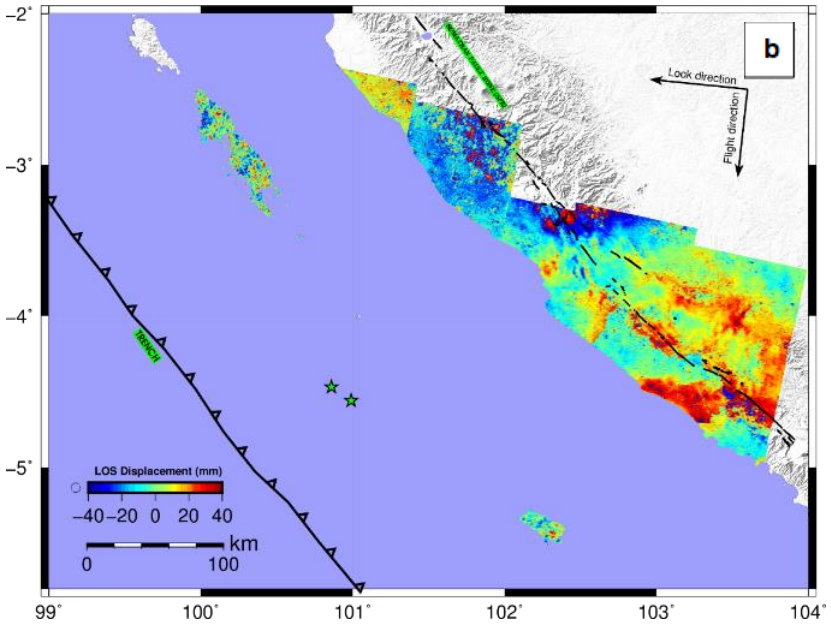

Figure 5. LOS displacement Bengkulu Earthquake August 18, 2020 (a) ascending direction (b) descending direction

CONCLUSIONS

In conclusion, this paper utilized coherence and interferogram analysis on pairs of satellite images before and after the Bengkulu coseismic earthquake on August 18, 2020. The Line of Sight (LOS) displacement was determined through unwrapping, allowing the identification of the deformation phenomenon. The results of Line of Sight (LOS) displacement in the ascending and descending satellite directions, respectively, ranged from ~-40 mm to ~40 mm. The InSAR data did not detect clear deformation patterns or displacements associated with the August 18, 2020 earthquake. However, it is crucial to acknowledge the impact of atmospheric disturbances and phase unwrapping on the coherence and interferogram formation during the coseismic phase. These findings contribute significantly to InSAR studies, particularly for small earthquakes in Indonesia, emphasizing the need for accurate assessments.

ACKNOWLEDGMENTS

The authors thank the European Space Agency for providing the Sentinel-1 SAR data used in this work. The map was created using Generic Mapping Tools (GMT) software (Wessel et al., 2013).

REFERENCES

Albano, M., Saroli, M., Montuori, A., Bignami, C., Tolomei, C., Polcari,

M., Pezzo, G., Moro, M., Atzori, S., Stramondo, S., & Salvi, S. (2018). The relationship between InSAR coseismic deformation and earthquake-induced landslides associated with the 2017 Mw 3.9 Ischia (Italy) earthquake. *Geosciences (Switzerland)*, *8*(8). https://doi.org/10.3390/geosciences8080303

Alif, S. M., Anggara, O., Perdana, R. S., Hasannah, U., & Azizah, F. N. (2024). Analysis Of Presumed Land Subsidence In The Cities Of Lampung Province Using InSAR And GNSS Data. Journal of Geoscience, Engineering, Environment, and Technology, 9(3), 287-293. https://doi.org/10.25299/jgeet.2024.9.3.14096

Alif, S. M., Anggara, O., Ristiana, V., & Engineering, G. (2023). *Jurnal Geografi Gea Coherence Analysis of Sentinel-1A Images in Various Land*. *23*(2), 135–143. https://doi.org/10.17509/gea.v23i2.61258

Alif, S. M., Fattah, E. I., Kholil, M., & Anggara, O. (2021). Source of the 2019 Mw6.9 Banten Intraslab earthquake modelled with GPS data inversion. *Geodesy and Geodynamics*, *12*(4), 308–314. https://doi.org/10.1016/j.geog.2021.06.001

Amani, M., Poncos, V., Brisco, B., Foroughnia, F., DeLancey, E. R., & Ranjbar, S. (2021). InSAR Coherence Analysis for Wetlands in Alberta, Canada Using Time-Series Sentinel-1 Data. *Remote Sensing*, *13*(16). https://doi.org/10.3390/rs13163315

Anggara, O., Rahadianto, M. A. E., Al Attar, M. N., Alif, S. M., Perdana, R. S., & Nugraha, A. W. Assessing Recent Land Subsidence in Bandar Lampung City, Indonesia through Time Series InSAR from 2015 to 2023. Jurnal Geografi Gea, 24(2), 195-204. https://doi.org/10.17509/gea.v24i2.71315

Anggara, O., Alif, S. M., Pratama, A. W., Melvin, W. (2024). Uji Signifikansi Stasiun GPS Kontinu dan Periodik dalam Identifikasi Pergerakan Koseismik. 13(1), 89–95. https://doi.org/10.25077/jfu.13.1.89-95.2024

Anggara, O., Welly, T. K., Fauzi, A. I., Alif, S. M., Perdana, R. S., Oktarina, S. W., Nuha, M. U., & Rosadi, U. (2023). Monitoring ground deformation of Sinabung volcano eruption 2018-2019 using DInSAR technique and GPS data. *AIP Conference Proceedings*, *2654*(February). https://doi.org/10.1063/5.0114428

Ardika, M., Meilano, I., & Gunawan, E. (2015). Postseismic deformation parameters of the 2010 M7.8 Mentawai, Indonesia, earthquake inferred from continuous GPS observations. *Asian Journal of Earth Sciences*, *8*(4), 127–133. https://doi.org/10.3923/ajes.2015.127.133

Chen, C. W., & Zebker, H. A. (2002). Phase unwrapping for large SAR interferograms: Statistical segmentation and generalized network models. *IEEE Transactions on Geoscience and Remote Sensing*, *40*(8), 1709–1719. https://doi.org/10.1109/TGRS.2002.802453

Dziewonski, A. M., Chou, T. A., & Woodhouse, J. H. (1981).

Determination of earthquake source parameters from waveform data for studies of global and regional seismicity. *Journal of Geophysical Research*, *86*(B4), 2825–2852. https://doi.org/10.1029/JB086iB04p02825

Fang, J., Xu, C., Wen, Y., Wang, S., Xu, G., Zhao, Y., & Yi, L. (2019). The 2018 Mw 7.5 Palu earthquake: A supershear rupture event constrained by InSAR and broadband regional seismograms. *Remote Sensing*, *11*(11). https://doi.org/10.3390/rs11111330

Funning, G. J., & Garcia, A. (2019). A systematic study of earthquake detectability using Sentinel-1 InterferometricWide-Swath data. *Geophysical Journal International*, *216*(1), 332–349. https://doi.org/10.1093/gji/ggy426

Goldstein, R. M. (1998). *Radar interferogram filtering for geophysical applications*. 1–9. https://doi.org/10.1029/1998gl900033

Jacob, A. W., Notarnicola, C., Suresh, G., Antropov, O., Ge, S., Praks, J., Ban, Y., Pottier, E., Mallorqui Franquet, J. J., Duro, J., Engdahl, M. E., Vicente-Guijalba, F., Lopez-Martinez, C., Lopez-Sanchez, J. M., Litzinger, M., Kristen, H., Mestre-Quereda, A., Ziolkowski, D., & Lavalle, M. (2020). Sentinel-1 InSAR Coherence for Land Cover Mapping: A Comparison of Multiple Feature-Based Classifiers. *IEEE Journal of Selected Topics in Applied Earth Observations and Remote Sensing*, *13*, 535–552. https://doi.org/10.1109/JSTARS.2019.2958847

Li, Y., Jiang, W., Zhang, J., Li, B., Yan, R., & Wang, X. (2021). Sentinel-1 SAR-Based coseismic deformation monitoring service for rapid geodetic imaging of global earthquakes. *Natural Hazards Research*, *1*(1), 11–19. https://doi.org/10.1016/j.nhres.2020.12.001

Meilano, I., Salman, R., Rahmadani, S., Shi, Q., Susilo, S., Lindsey, E., Supendi, P., & Daryono, D. (2021). Source Characteristics of the 2019 Mw 6.5 Ambon, Eastern Indonesia, Earthquake Inferred from Seismic and Geodetic Data. *Seismological Research Letters*, *92*(6), 3339–3348. https://doi.org/10.1785/0220210021

Monterroso, F., Bonano, M., Luca, C. De, Lanari, R., Manunta, M., Manzo, M., Onorato, G., Zinno, I., & Casu, F. (2020). A Global Archive of Coseismic DInSAR Products Obtained Through Unsupervised Sentinel-1 Data Processing. *Remote Sensing*, *12*(19). https://doi.org/10.3390/rs12193189

Mora, O., Ordoqui, P., Iglesias, R., & Blanco, P. (2016). Earthquake Rapid Mapping Using Ascending and Descending Sentinel-1 TOPSAR Interferograms. *Procedia Computer Science*, *100*, 1135–1140. https://doi.org/10.1016/j.procs.2016.09.266

Natadikara, R., Fauzi, A. I., Anggara, O., Perdana, R. S., Alif, S. M., Julzarika, A., Nurtyawan, R., & Rohman, A. (2023). Monitoring Deformation of Anak Krakatoa Volcano Using Differential Interferometry Synthetic Aperture Radar (DInSAR) Method. *AIP Conference Proceedings*, *2941*(1). https://doi.org/10.1063/5.0181540

PuSGeN. (2017). *Peta sumber dan bahaya gempa Indonesia tahun 2017*. Pusat Penelitian dan Pengembangan Perumahan dan Permukiman Badan Penelitian dan Pengembangan Kementerian Pekerjaan Umum dan Perumahan Rakyat.

Sandwell, D., Mellors, R., Tong, X., Xu, X., Wei, M., & Wessel, P. (2010). GMTSAR Software for Rapid Assessment of Earthquakes. *AGU Fall Meeting Abstracts*.

Suresh, D., & Yarrakula, K. (2020). InSAR based deformation mapping of earthquake using Sentinel 1A imagery. *Geocarto International*, *35*(5), 559–568. https://doi.org/10.1080/10106049.2018.1544289

Tanioka, Y., Yudhicara, Kususose, T., Kathiroli, S., Nishimura, Y., Iwasaki, S. I., & Satake, K. (2006). Rupture process of the 2004 great Sumatra-Andaman earthquake estimated from tsunami waveforms. *Earth, Planets and Space*, *58*(2), 203–209. https://doi.org/10.1186/BF03353379

Vigny, C., Simons, W. J. F., Abu, S., Bamphenyu, R., Satirapod, C., Choosakul, N., Subarya, C., Socquet, A., Omar, K., Abidin, H. Z., & Ambrosius, B. A. C. (2005). Insight into the 2004 Sumatra-Andaman earthquake from GPS measurements in southeast Asia. *Nature*, *436*(7048), 201–206. https://doi.org/10.1038/nature03937

Wessel, P., Smith, W., Scharroo, R., Luis, J., & Wobbe, F. (2013). Generic Mapping Tools: Improved Version Released. *Eos Transactions American Geophysical Union*, *94*. https://doi.org/10.1002/2013EO450001

Yang, C., Han, B., Zhao, C., Du, J., Zhang, D., & Zhu, S. (2019). Co- and post-seismic Deformation Mechanisms of the MW 7.3 Iran Earthquake (2017) Revealed by Sentinel-1 InSAR Observations. *Remote Sensing*, *11*(4). https://doi.org/10.3390/rs11040418

Yu, C., Li, Z., Chen, J., & Hu, J. C. (2018). Small magnitude coseismic deformation of the 2017 Mw 6.4 Nyingchi earthquake revealed by InSAR measurements with atmospheric correction. *Remote Sensing*, *10*(5). https://doi.org/10.3390/rs10050684

Zhao, D., Qu, C., Shan, X., Gong, W., Zhang, Y., & Zhang, G. (2018). InSAR and GPS derived coseismic deformation and fault model of the 2017 Ms7.0 Jiuzhaigou earthquake in the Northeast Bayanhar block. *Tectonophysics*, *726*, 86–99. https://doi.org/https://doi.org/10.1016/j.tecto.2018.01.026